AIAA JOURNAL
Vol. 45, No. 3, March 2007

Effect of Co- and Counterswirl on Noise from Swirling Flows and Flames

Kapil K. Singh, Luc Mongeau, Steven H. Frankel, and Jay P. Gore*
Purdue University, West Lafayette, Indiana 47907-2040

DOI: 10.2514/1.14057

Overall and spectral sound pressure levels radiating from swirling flows and flames were measured and correlated with simultaneous plenum pressure fluctuations measurements. Single swirler and co- and counter-rotating double swirlers were used. Generic radial-entry swirlers with straight vanes and a convergent–divergent nozzle were employed. At the same Reynolds number and Mach number, precessing-vortex-core frequency, spectral amplitude at that precessing-vortex-core frequency, and overall sound pressure levels for flows were the highest for the single swirler, followed by the co- and counter-rotating double swirlers. Rates of increase in precessing-vortex-core frequency and overall sound pressure levels with Reynolds number and Mach number were also in the same order. Sound spectra for single and corotating double swirlers contained precessing-vortex-core-related strong tonal components. However, for counter-rotating double-swirler flows, amplitude of the tonal component was reduced considerably. Double-swirler configurations exhibited dual precessing-vortex-core frequencies. The addition of a second swirler slowed down precessing-vortex-core and reduced its upstream transmission to the plenum and the transmission of plenum modes to the sound field. The counter-rotation configuration was more effective in slowing down the precessing vortex core and acting as a transmission barrier than the corotation configuration. Compared to flow, partially premixed flame, $\Phi = 1.15$, produced 5–10 dB higher overall sound pressure levels. However, the flame had a lower Mach number exponent than the flow. Flames inhibited the transmission of high-frequency tones across them. At the same Φ and Reynolds number, the corotating flame was the least noisy and the counter-rotating flame was the noisiest. Premixed flames with $\Phi = 0.98$ were compared with the flows by keeping an identical pressure differential across the premixer. The counter-rotating double swirlers produced higher overall sound pressure levels than the corotating double swirlers, which generated more overall sound pressure levels than the single swirler.

Introduction

MANY gas turbine engines for propulsion systems feature swirl combustors to achieve stable, efficient, and clean combustion [1–4]. Swirl combustors feature complex unsteady reacting flow, thermal, and species fields [5–13]. Swirling flows often exhibit instabilities characterized by vortex breakdown and the emergence of a precessing vortex core [14] (PVC). The PVC is a naturally occurring three-dimensional time-dependent hydrodynamic instability that rotates about the central vortex core axis. This phenomenon has been the subject of various investigations [1–3,7,11,15]. The combustion dynamics in such systems are caused by interactions between the unsteady heat release with the temporal and spatial unmixedness and the unsteady fluid mechanical phenomena of PVC and vortex breakdown. The PVC is altered by these interactions [16–19] and may also, in turn, modify the combustion processes [20–23]. Premixed combustion excites the PVC to higher frequencies and intensities than those of the isothermal flow; whereas diffusion-controlled combustion suppresses the PVC intensities by two orders of magnitude [17]. This damping is primarily caused by a decrease in swirl number, due to the axial acceleration of the flow by the combustion process [19]. The PVC was also damped by axial and tangential entry natural gas flames, due to large radial density gradients, but it was still detected on the boundary of the reverse flow zone [17]. Recently, the presence of a PVC in a natural gas lean flame, with an equivalence ratio of $\Phi = 0.887$, has been reported for a wide range of swirl characteristics [23]. The PVC is characterized by periodic fluctuations of flow velocity, pressure, and temperature. The heat release rate oscillates nearly in phase with pressure. The pressure oscillations may couple to, and get amplified by, the natural acoustic modes of the combustor, leading to feedback-loop-type combustion instabilities [24,25]. Using bluff-body-type stabilization, the plenum and flame zone pressure fluctuations and flame zone and exit pressure fluctuations for an enclosed flame have been found to be very coherent [26]. The sources of noise in a swirl burner can be broadly classified as aerodynamic or turbulence-generated noise, combustion-driven oscillations, combustion noise, and resonant coupling with one of the modes of enclosure. Combustion-driven oscillations are generally linked to system, acoustical, and transition instabilities. Resonant coupling can be witnessed in flows with a strong degree of swirl [27]. Combustion noise is generated by the unsteady characteristics of the turbulent combustion process [28–30]. The sound-generation mechanism is a function of the rate of change of the heat release rate and does not depend on the actual heat release rate [31].

Gupta et al. [32] measured radiated noise spectra of swirl-stabilized natural gas flames for various flow rates, air–fuel ratios, and modes of fuel injection. The source of sound was the region of maximum pressure fluctuations. A reduction in the noise emissions was observed when this region was surrounded by a second outer flame boundary. Equal division of fuel between the axial and radial inlets was suggested for a low-noise stable swirl burner. The convergent–divergent exit nozzle significantly increased noise levels, compared with straight exit nozzles. Bertrand and Michelfelder [33] measured the sound power emitted by a natural-gas-fired experimental burner both in free-field conditions and inside a refractory furnace. The emissions inside the furnace illustrated the predominance of resonant modes at low frequencies. The sound power output increased with the 2.8th power of average gas velocity and the 5.6th power of the throat diameter. The peak frequency of combustion was a function of the swirl number and independent of the firing rate of the burner. Preheating of the oxidizer (air) greatly increased the sound power output and the peak frequency of emitted noise spectra. Gupta et al. [34,35] investigated the noise generated by a laboratory-type burner with swirl numbers of around two. Under

Received 19 October 2004; revision received 28 November 2006; accepted for publication 12 November 2006.

*School of Mechanical Engineering, 585 Purdue Mall; gore@ecn.purdue.edu.

nonreacting flow conditions, the PVC dominated the flowfield and was the main source of sound. Under reacting flow conditions and for the same burner loading, sound levels for a tangential fuel inflow were lower than those for an axial fuel inflow. The burners discharging through a convergent–divergent nozzle were the noisiest, although at high flow rates, the effects of the nozzle geometry on the radiated noise level were insignificant. Overall noise reduction was achieved through staged combustion. Gupta et al. [3] have also reported that diffusion flames are noisier than premixed flames. Hardalupas and Selbach [36] imposed oscillations on the coaxial air flow of a swirl-stabilized burner with natural gas injected axially and radially in the center of the flow, with and without a diffuser at the burner exit. This improved the lean-flammability limits of the burner. Neemeh et al. [37] used a swirl chamber to investigate the effect of fluid rotation on the noise generated by supersonic jets. Small flow rotation reduced the generated noise, but higher fluid rotation had no additional effect. Recently, Nair and Lieuwen [38] demonstrated use of acoustic measurements to detect imminent blowout in pilot- and swirl-stabilized combustors. The low-frequency spectra exhibited a strong dependence upon the degree of flame stabilization.

The use of two or more swirlers with concentric annuli offers additional control on the swirl characteristics, and significantly different flow and mixing patterns can be achieved. A substantial reduction in NO_x emissions through the use of multi-annular swirl burners [39] has been reported. A similar reduction was also found by use of the double-swirler burner in comparison with the single-swirler burner [40]. The counterswirl burners exhibited stronger radial exchange, compared with the coswirl burner [21]. The counterswirl configuration increased the flame stability, compared with the coswirl configuration [41,42]. The effects of the co- and counterswirling configurations on the flowfield [9,42,43] and thermal characteristics [44] have also been studied.

The differences in sound generation from swirling flames and flows are not yet completely understood. Also, the effect of co- and counter-rotating double swirlers on the sound generation of reacting and nonreacting swirling flows has not been investigated. The specific objectives of this study were to 1) compare the overall and spectral sound pressure levels (OASPL) and sound spectra generated by swirling flames with those of nonreacting swirling flows under identical conditions; 2) investigate the effect of the PVC on the plenum pressure fluctuation spectra and the emitted sound spectra; 3) compare the Mach number scaling of the OASPL generated by swirling flames with that of nonreacting swirling flows; 4) study the correlation of internal plenum pressure fluctuations and external sound measurements; 5) measure the sound pressure radiated from swirling flames and flows to understand the effects of co- and counter-rotating double swirlers on noise emissions; and 6) characterize the sound pressure spectra and plenum pressure fluctuations spectra as a function of the Reynolds number.

Experimental Apparatus

The experiments were conducted in a lean premixed combustor facility, shown schematically in Fig. 1a. Also shown is a picture of the flame with $\Phi = 0.98$. The facility is installed in an enclosure with the dimensions of 1.3 m (length) × 1.2 m (width) × 3.0 m (height), with an exhaust hood at the top. The premixer design is known as the radial swirler plus nozzle (RSPN) and is the result of the Allison Engine Company's advanced turbine system (ATS) development program, in collaboration with the U.S. government's Department of Energy (DOE) [45]. The premixer with swirlers was assembled on a plenum, which supplies air and fuel to the premixer. The plenum was mounted on a three-dimensional traverse system. A buffer plate was installed inside the plenum to create a uniform upstream airflow. The air was supplied through the bottom and directly into the plenum. The fuel (methane) was supplied to the bottom of the swirler premixer. Table 1 provides details of test conditions and results at end points of the test Reynolds number range for all three swirler configurations studied, with a constant increment in Reynolds number of 3000. A schematic diagram of the radial swirlers used in this study is shown in Fig. 1b. The swirling premixer was made up of four main parts: nozzle head, upper swirler, lower swirler, and base plate. The details of the premixer-nozzle assembly are depicted in Fig. 2a. The nozzle throat diameter was $D_t = 3.81$ cm and the exit diameter was $D_e = 8.64$ cm. Both swirlers had an inner diameter of 5.08 cm, with 16 straight vanes. The upper swirler was 28.8-mm long and the lower swirler was 7.6-mm long. The blade angle was 21 deg. The lower swirler could be installed with different orientations to form corotating or counter-rotating double swirlers. The design drawing of the nozzle is provided in Fig. 2b. The detailed drawings of all other components are available in [46]. The swirl intensity is characterized in terms of the swirl number S, defined as [3]

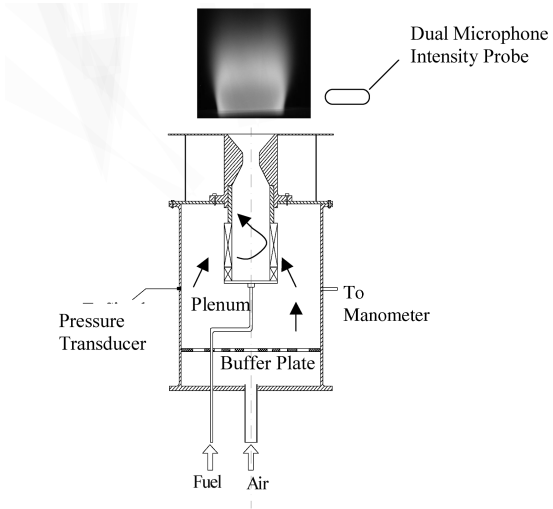

a) Experimental arrangement with flame picture

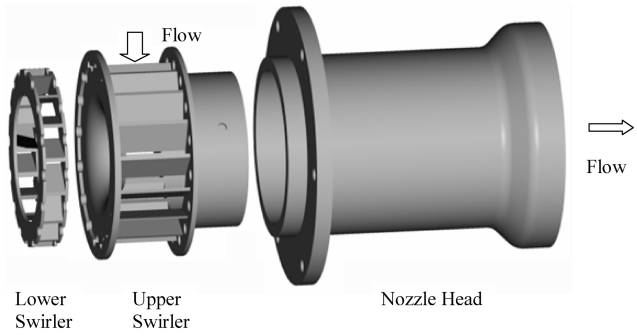

b) Nozzle and swirler configuration

Fig. 1 Experimental apparatus.

$$S = \left(\frac{2}{D_{\mathrm{SW}}}\right)\left(\frac{G_\theta}{G_x}\right) \tag{1}$$

where D_{SW} is the inner diameter of the swirler, G_θ is the axial flux of angular momentum, and G_x is the axial flux of axial momentum. For the single-swirler configuration, the theoretical swirl number at the exit of the swirler was estimated [10] to be 2.4.

A miniature integrated circuit piezoelectric (ICP) pressure transducer (PCB model 112A22) was mounted on the sidewall of the air plenum chamber to measure pressure fluctuations. The pressure transducer had a resolution of 6.9 Pa, its resonant frequency was 250 kHz, and its cut-on frequency was 0.50 Hz, with a rise time of 2 ms. A pressure transducer signal conditioner (PCB model 482B11) was used. The frequency response of the signal conditioner was uniform up to 100 kHz, within 1%. The radiated sound pressure measurements were made using a microphone from a Bruel & Kjaer 3599 Intensity Probe, which included a phase-matched pair of 1.27-cm-diam (1/2-in.) Bruel & Kjaer 4197 condenser microphones. The output signals from the transducers were fed to a two-channel Siglab, model 20-22A, a PC-based data acquisition and analysis system. The system was capable of acquiring data up to a sampling rate of 50 kHz, with anti-aliasing filters and different time-domain windows. The

Table 1 Details of test conditions and results for all three swirler configurations

Serial no.	Swirler configuration	Reynolds no.	Mass flow, kg/min		Equiv. ratio	Throat vel., m/s	Mach no.	PVC tone, Hz	St_{ch}
			Air	Fuel					
1	Single swirler	35,000	1.144	——	——	13.95	0.041	285	0.79, 1.58
2		80,000	2.640	——	——	32.10	0.094	645	
3		51,000	1.503	0.101	1.15	20.52	0.060	——	——
4		81,000	2.390	0.162	1.15	32.66	0.096	——	
5	Corotating	45,000	1.488	——	——	18.13	0.053	315	0.17, 0.64, 1.28
6	double swirlers	99,000	3.264	——	——	39.75	0.116	655	
7	Counter-rotating	80,000	2.635	——	——	32.10	0.094	315	0.11, 0.43
8	double swirlers	116,000	3.816	——	——	47.15	0.139	545	

same system was used for spectral analysis, including autospectrum, cross-spectrum, and coherence. All external sound measurements were made at one far-field location approximately $r/D_t = 9$ and $x/D_t = 1$ away from the combustor. A Hanning time-domain window was used. The data acquisition rate was 2.56 times the highest frequency of interest. For spectral measurements up to 10 kHz, the sampling rate was 25.6 kHz, whereas for 2 kHz, the sampling rate was 5.12 kHz; 1024 points were collected and 300 averages were made for each measurement. The pressure difference across the swirling premixer was measured using a manometer connected to the sidewall of the plenum. This study was conducted in a nonanechoic facility by design, to simulate conditions closer to the nonideal conditions encountered in both aircraft engines and land-based gas turbines. The measurements were close enough to the sources to ensure the dominance of the direct field instead of the reverberant field. This was validated by measuring the sound generated by a Bruel & Kjaer type 4204 reference source under laboratory conditions. The measured spectra and OASPL were comparable to specified values within experimental uncertainties of ± 2 dB, as shown in Fig. 3.

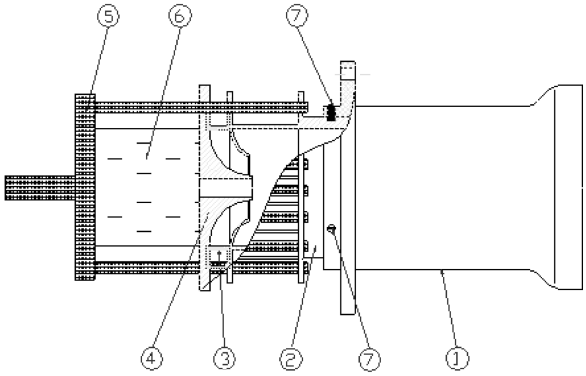

1. Nozzle Head; 2. Upper Swirler; 3. Lower Swirler;
4. Base Plate; 5. Fuel Manifold; 6. Spacer; 7. Screws

a) Details of premixer-nozzle assembly

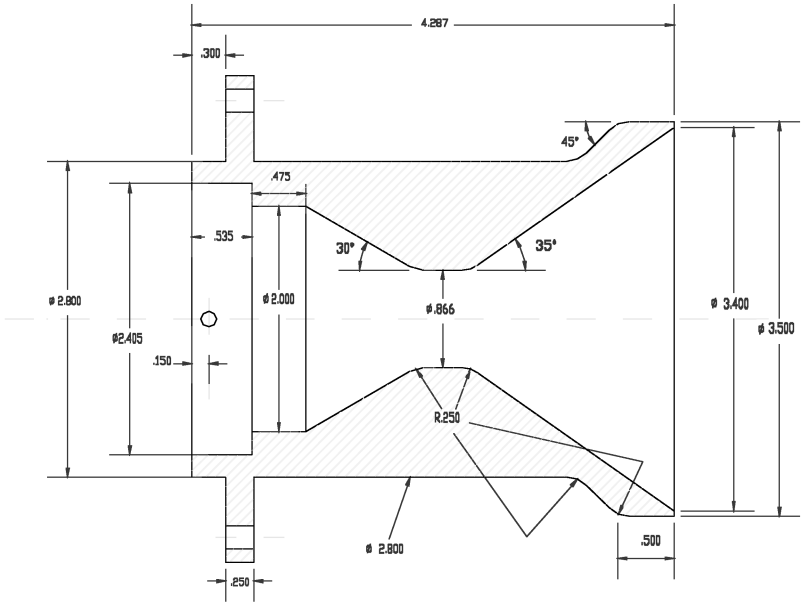

b) Nozzle design drawing

Fig. 2 ATS premixer.

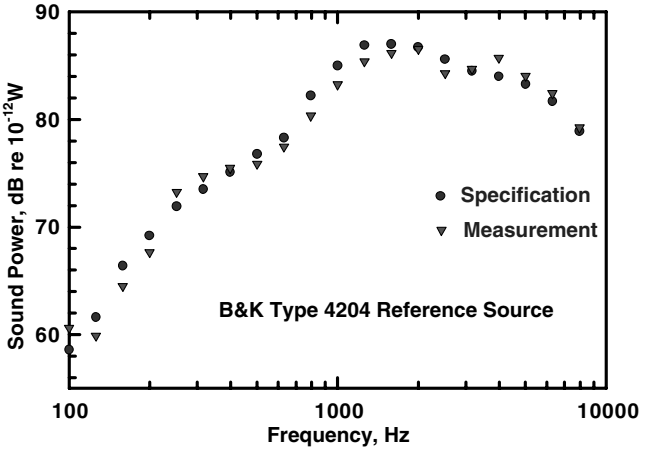

Fig. 3 Comparison of measurements of the Bruel & Kjaer type 4204 reference source in laboratory conditions with manufacturer's specifications ($r/D_t = 9$ and $x/D_t = 1$).

Results and Discussion

Figure 4a shows the variation of the PVC-related tonal frequency components as a function of the Reynolds number ($Re = U_t D_t/\nu$, where U_t is average overall throat velocity and ν is kinematic viscosity) for single, co-, and counter-rotating double-swirler nonreacting flows. The PVC is a phenomenon associated primarily with high-swirl-number ($S > 0.6$) flows, and it appears only after vortex breakdown and the formation of recirculation zones and, thus, is a function of the Reynolds number. The lowest Reynolds number in Fig. 4a corresponds to the appearance of a PVC for that specific swirler arrangement. For nonreacting swirling flows, the PVC-related tonal frequency dominates the spectra with its very high amplitude and is thus identified. A linear increase in peak frequency was observed for all configurations, confirming that these dominant tonal components are due to the PVC. At the same Reynolds number, the PVC frequency is the highest for the single swirler, followed by corotating double swirlers, and the lowest for counter-rotating double swirlers. The rate of increase in the PVC frequency is also different for various configurations, with the highest rate for the single swirler, followed by corotating double swirlers, and the least for counter-rotating double swirlers. Both corotating and counter-rotating double-swirler arrangements exhibit a second PVC tone. Recently, the presence of a double PVC has been reported for premixed and nonpremixed flames [23]. The two PVC frequencies with double swirlers exhibit a lack of complete mixing of the two streams emanating from the two swirlers. These can be correlated to the dimensions of the upper and lower swirlers, with the direction of the rotation taken into account [46]. The precession frequency of the PVC is known to be low and in the range of 10–200 Hz [3,16,17]. It is believed that the observed PVC frequency in the sound spectra is related to its precession frequency through the number of vanes (i.e., PVC frequency = precession frequency × number of vanes).

Figure 4b shows the OASPL as a function of the Mach number ($M = U_t/C_{\text{air}}$, where C_{air} is the speed of sound in ambient air) for nonreacting swirling flows using single, co-, and counter-rotating double swirlers, and for a swirling partially premixed flame at $\Phi = 1.15$ using the single swirler. For evaluating the effect of the Mach number and Reynolds number on the spectra and OASPL of

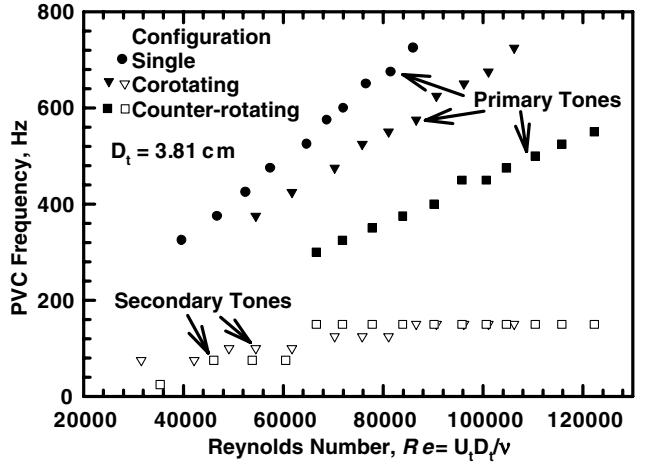

a) Variation of PVC frequency with the Reynolds number

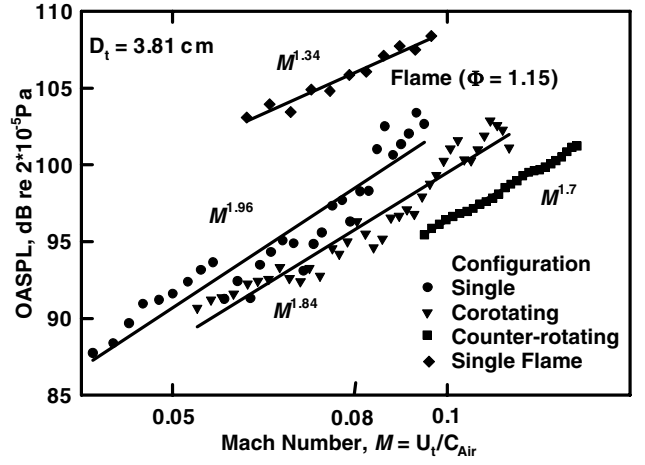

b) Variation in OASPL with the Mach number

Fig. 4 Swirler configuration effects for three swirler configurations ($r/D_t = 9$ and $x/D_t = 1$).

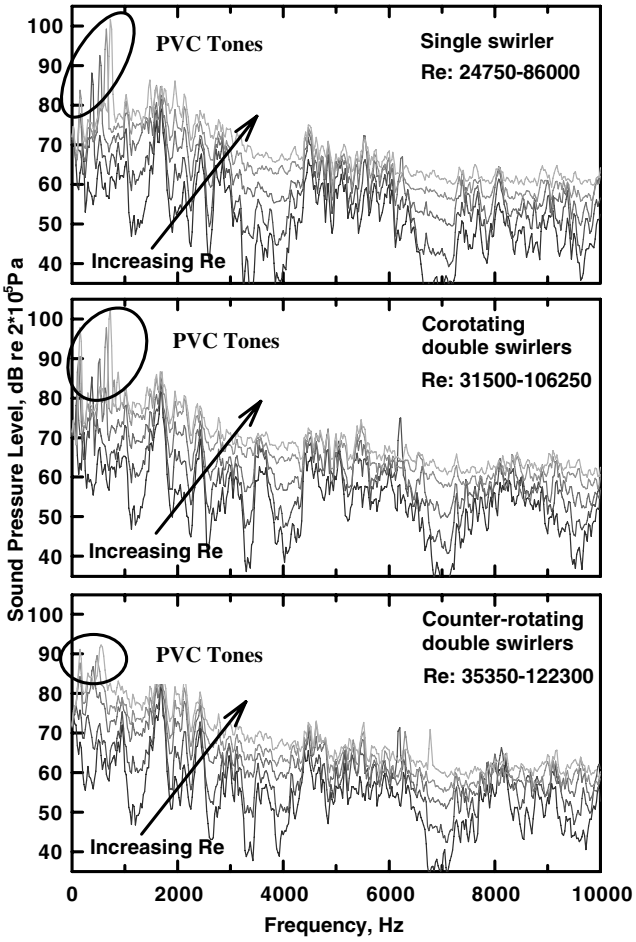

Fig. 5 Effect of Reynolds number variation on the sound pressure spectra of swirling flows for three swirler configurations ($r/D_t = 9$ and $x/D_t = 1$).

the single-swirler flame, the choice of equivalence ratio was governed by the need to have stable flames over the Reynolds number range in the partially premixed regime. The OASPL is obtained from the spectra by integration. The sound generated by nonreacting flows is known to scale with the Mach number. Hence, the PVC frequency is represented as a function of the Reynolds number, whereas the OASPL is represented as a function of the Mach number. A linear regression analysis was applied to all cases and the Mach number scaling exponents were obtained for sound pressure. The sound pressure generated by the single-swirler nonreacting flow exhibits the highest exponent ($M^{1.96}$) among nonreacting flows, followed by corotating double swirlers ($M^{1.84}$), and the counter-rotating double-swirlers nonreacting flow has the lowest exponent ($M^{1.7}$). The single-swirler partially premixed flame with $\Phi = 1.15$ generates 5–10 dB higher OASPL than the single-swirler nonreacting flow, with the difference reducing with increase in the Mach number. However, the flame exhibits a lower exponent of $M^{1.34}$, compared with $M^{1.96}$ for the nonreacting swirling flow. This finding is similar to the premixed jet flames exhibiting a lower exponent, compared with the nonreacting jet [47], but is different from comparable exponents of the nonpremixed jet flames and the nonreacting jets [48].

Figure 5 shows the variation in sound pressure spectra of nonreacting swirling flows with increase in velocity/Reynolds number for all three different configurations. The bandwidth was 10 kHz, the frequency resolution was 25 Hz, and the sampling frequency was 25.6 kHz. The amplitude at the PVC frequency is the highest for the single-swirler arrangement, followed by the coflow double swirler, and the least for the counterflow double-swirler arrangement. At lower Reynolds numbers, the spectral component (at about 1700 Hz) dominates the sound spectra for all configurations, and as the Reynolds number increases, it is overtaken by the PVC tone. However, this characteristic differs among the various configurations, including when it is overtaken and its relative amplitude. Three different types of systematic behavior can be observed in the spectra of all swirler configurations: 1) gradual increase in frequency associated with increase in the amplitude at that frequency (between frequencies of 300–800 Hz), which is attributable to the PVC; 2) gradual increase in amplitude at a constant frequency (at around 1200, 2700, 3400, 4000, and 7000 Hz); and 3) constant amplitude at a constant frequency (at around 1700, 2400, 4400 Hz, etc.).

To understand the origin of these features, simultaneous measurements of internal pressure fluctuations and external far-field sound [with systematic constant increase in flow velocity (Reynolds number)] were completed. Narrowband spectra with a frequency resolution of 5 Hz and bandwidth of 2 kHz were obtained at the sampling frequency of 5.12 kHz to concentrate on the low-frequency region dominant in the spectra. These measurements were obtained with a constant increment of $Re = 3000$ for all three configurations. The range of Reynolds number was selected to have PVC frequencies in a similar range. Figure 6 presents the systematic variation in the spectra of nonreacting swirling flows for all configurations, with a constant incremental, gradual increase in Reynolds number. For clarity, only spectra with a Reynolds number difference of 9000 are displayed. The first harmonic of the PVC can be distinctly seen in the spectra for the single and corotating double swirlers. Very similar constant frequency features can be seen in all the spectra. The constant amplitude components, with the most dominant component at about 1700 Hz, are present in all three swirlers.

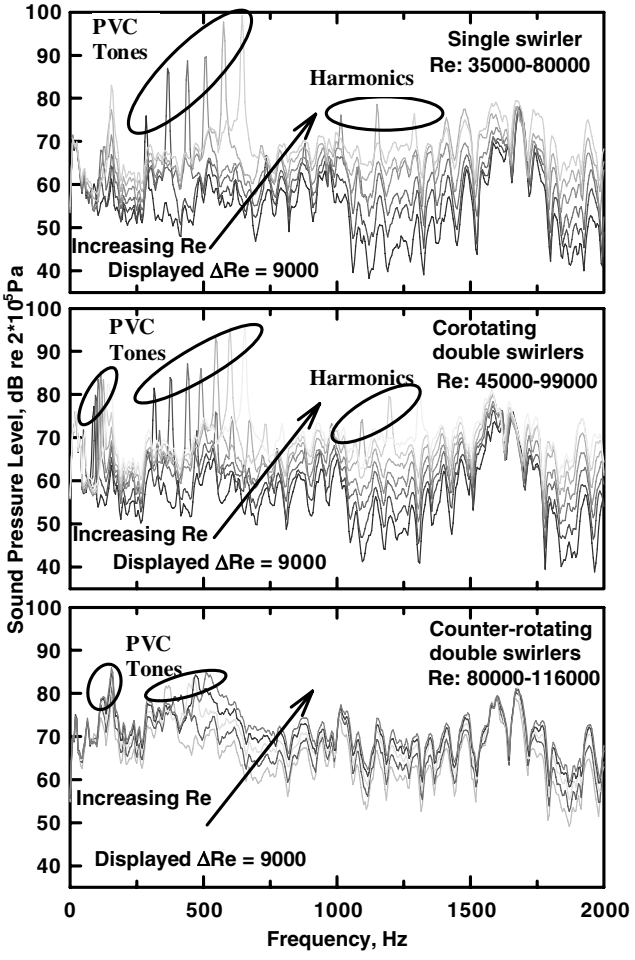

Fig. 6 Effect of Reynolds number variation on the sound pressure spectra of swirling flows for three swirler configurations with a constant Reynolds number increment of 3000 ($r/D_t = 9$ and $x/D_t = 1$).

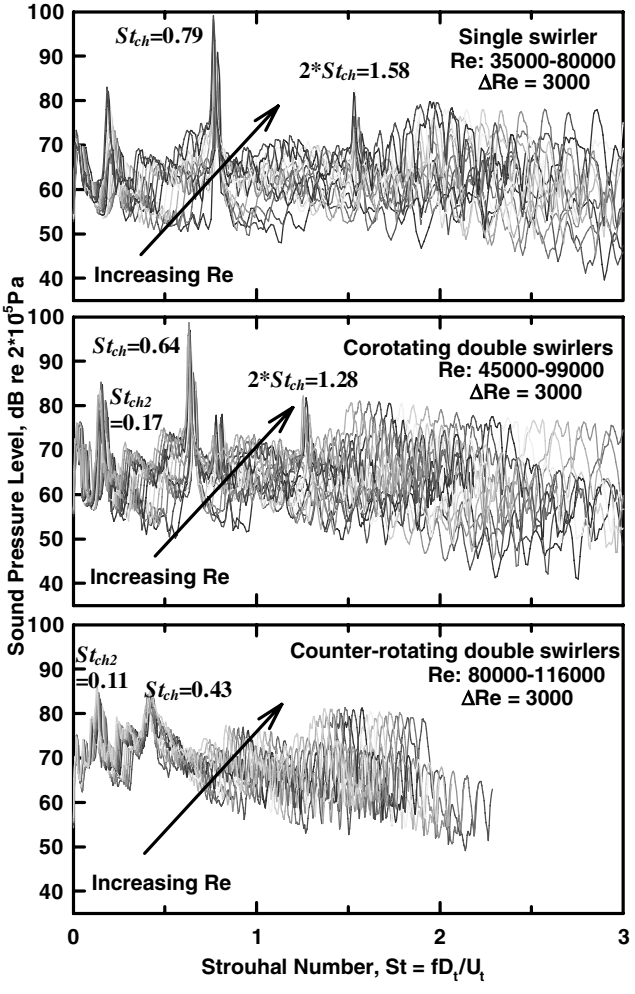

Fig. 7 Sound pressure spectra of Fig. 6 as a function of the Strouhal number ($r/D_t = 9$ and $x/D_t = 1$).

Figure 7 presents the same spectra as in Fig. 6 as a function of the Strouhal number ($St = fD_t/U_t$, where f is the frequency) with increase in the Reynolds number. The gradually increasing frequencies collapse well at one Strouhal number, confirming that these frequencies are proportional to velocity. However, the fixed frequency components are spread out. The Strouhal number at which PVC frequencies collapse is defined as the characteristic Strouhal number St_{ch}, and this is a property of that specific swirler arrangement [46]. The characteristic Strouhal number (St_{ch} for the single swirler) is 0.79, which is lowered to 0.64 by the addition of a second swirler with corotation and further reduced to 0.43 with counter-rotating double swirlers. Therefore, the addition of a second swirler slows down the PVC, with counter-rotation having a stronger effect. The fluid coming in from the lower swirler acts as a resistance to the rotation of the fluid coming in from the upper swirler, and this resistance is increased further when the direction of rotation is reversed. The second PVC tones generate a second characteristic Strouhal number (St_{ch2} for double swirlers) at 0.17 for corotating double swirlers and 0.11 for counter-rotating double swirlers. Also visible are the first harmonics of St_{ch} at 1.58 and 1.28 for single and corotating double swirlers, respectively. In addition, the St_{ch} for the single swirler at 0.79 can still be observed for corotating double swirlers. This suggests that the resistance offered by the corotating lower swirler does not impact the single-swirler flowfield completely, and as shown by Ji and Gore [10], the flowfields of single and corotating swirlers are very similar. The peak observed for the single swirler in Fig. 6 (around 150 Hz) is constant frequency, as can be seen in the spread observed in Fig. 7. In addition to the spectra depicted, data values of frequency and peak were extensively analyzed to clearly deduce the distinction in the constant frequency of the single swirler in comparison with the variable frequency behavior of double-swirler configurations. Table 1 also summarizes the results from the systematic variation in the spectra.

Table 2 Natural modes of the plenum cylinder

m	q	η_{qm}	Frequency, Hz
0	1	0.000	0
	2	3.832	1282
	3	7.016	2347
1	1	1.841	613
	2	5.331	1783
	3	8.536	2856
2	1	3.054	1022
	2	6.706	2243
	3	9.969	3335

Figure 8 presents the spectra of plenum pressure fluctuations with increase in Reynolds number for all three configurations. These are simultaneous measurements with the sound spectra of Fig. 6. The plenum pressure fluctuations are represented as dB, with the same reference pressure of 20 μPa used for sound. The plenum pressure fluctuations spectra differ substantially from the external sound spectra. The PVC-linked features can still be seen in the single-swirler spectra and are discernible in some corotating double-swirler spectra. However, counter-rotating spectra are noticeably devoid of any PVC features.

The eigenfunctions for a duct with a circular cross section are given by [49,50]

$$\Psi_n(r,\theta) = K_{qm} J_m\left(\frac{\eta_{qm} r}{a}\right)\left\{\begin{matrix}\cos(m\theta)\\ \sin(m\theta)\end{matrix}\right\} \tag{2}$$

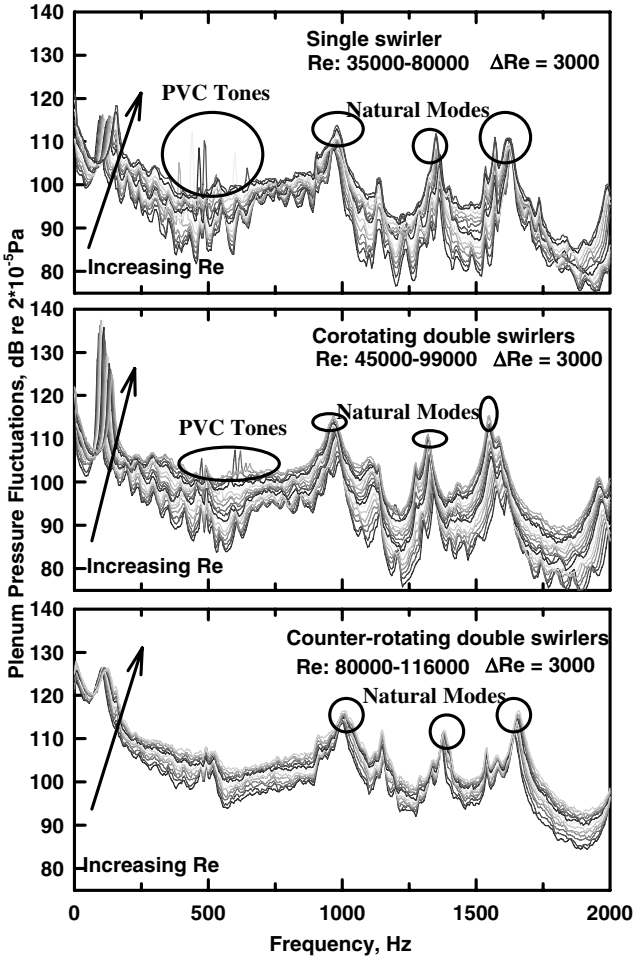

Fig. 8 Effect of Reynolds number variation on the plenum pressure fluctuation spectra of swirling flows for three swirler configurations with a constant Reynolds number increment of 3000 ($r/D_t = 9$ and $x/D_t = 1$).

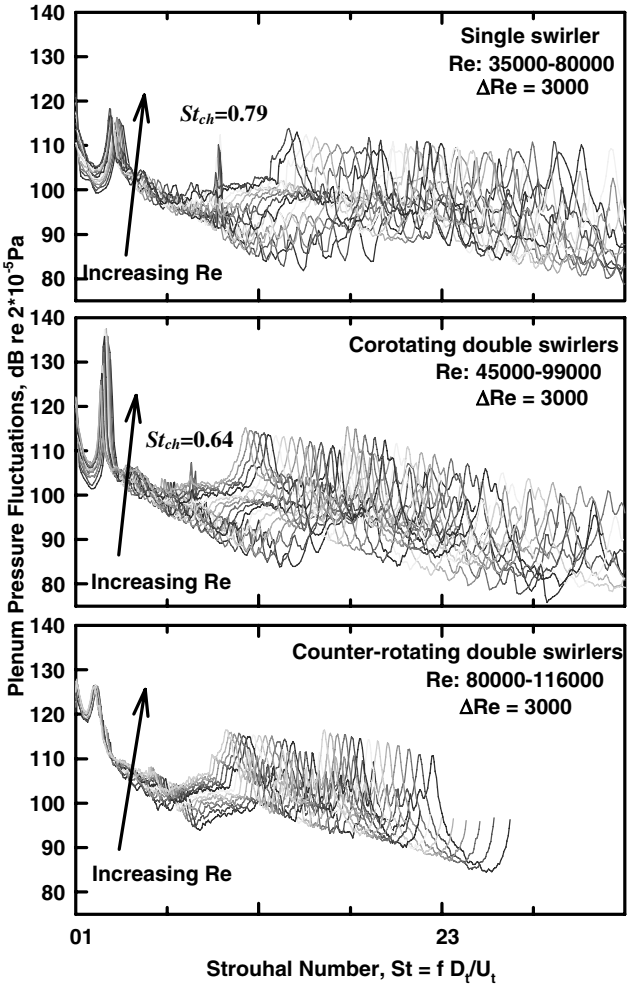

Fig. 9 Plenum pressure fluctuations spectra of Fig. 8 as a function of the Strouhal number ($r/D_t = 9$ and $x/D_t = 1$).

where η_{qm} denotes the qth root of $\eta_{qm}J'_m(\eta_{qm}) = 0$, J_m is the Bessel function of order m, r and θ are radial and tangential coordinates, K_{qm} is a constant, and a is the radius of the duct. The natural modes of the premixer cylinder, neglecting the presence of the swirlers, were calculated and are summarized in Table 2. The frequencies around 1020, 1280, and 1780 Hz are the most dominant modes and are visible in the spectra for all configurations. The peak in the 150–250 Hz range is a system frequency that is possibly linked to the air system. This is the same tone that is observed in the external spectra of the single-swirler configurations. However, as demonstrated later, the introduction of a second swirler inhibits the transmission of system/plenum frequencies to the external sound field; thus, this tone is not seen in external sound measurements of double swirlers. Figure 9 presents the same spectra as in Fig. 8 as a function of the Strouhal number. The St_{ch} for the single swirler at 0.79 can be clearly observed. Also, the St_{ch} for corotating double swirlers is discernible at 0.64, but for the counter-rotating double swirlers, the St_{ch} at 0.43 is noticeably absent. The St_{ch2} for double swirlers is also not present in the plenum pressure fluctuation spectra. However, the spectral feature of increase in amplitude at constant frequency is present in the spectra of all swirlers.

Figure 10 shows the coherence between the plenum pressure fluctuations and the external sound for the three swirlers as a function of the frequency at various Reynolds numbers. Coherence is calculated as the cross-correlation between the two signals (internal pressure transducer and external microphone) and normalized using the autocorrelations of both signals. The strong coherence at frequencies around 1020 and 1780 Hz can be seen in all swirlers. Though the coherence levels at a frequency of around 1020 Hz are comparable for all swirlers, a reduction in coherence at around 1780 Hz can be observed from single to corotating double to counter-rotating double swirlers. In addition, the similarities in the signals reduce from single to corotating to counter-rotating double swirlers. The introduction of a second swirler acts as a shield to the downstream transmission of plenum pressure fluctuations, with counter-rotation having a stronger impact. The coherence as a function of the Strouhal number is presented in Fig. 11. The St_{ch} at 0.79 for the single swirler is distinctly visible. The presence of St_{ch} for corotating double swirlers at 0.64 is barely discernible and the St_{ch} for counter-rotating double swirlers at 0.43 is totally absent. Therefore, the double-swirler configurations act as a barrier for the upstream transmission of the PVC, with counter-rotation having a stronger effect.

Figure 12 shows the variation in sound spectra with the Reynolds number for the single-swirler partially premixed flame with $\Phi = 1.15$. The peak tone frequency was found to be invariant with respect to the Reynolds number. And the increase in frequency associated with increase in amplitude, a feature linked to the PVC, was observed in the 1200–1300 Hz frequency range, about four times higher than the corresponding frequency range for a nonreacting flow. This confirms the earlier observations of the shifting of the PVC frequency by two to four times by combustion [17]. The attempts to find St_{ch} for the flame were obscured by high-amplitude, low-frequency constant tones. Also, the plenum mode spectral feature at around 1700 Hz is conspicuously absent. Combustion noise is known to be low-frequency [32,51], and the frequency of the dominant peak, which remains invariant with respect to the Reynolds number, appears to be a manifestation of the fuel used and the hardware employed. Further experiments and a different approach are required to understand the behavior of swirling flames [46]. Therefore, the Reynolds-number-dependence study for corotating and counter-rotating flames was not conducted.

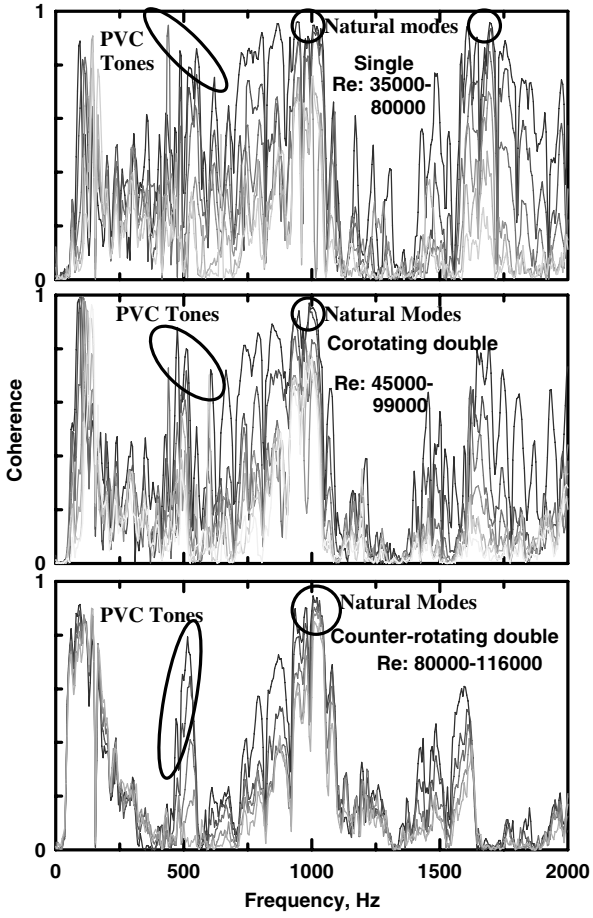

Fig. 10 Coherence between plenum pressure fluctuations and sound spectra as a function of the frequency for variations in Reynolds numbers ($\Delta Re = 3000$) for three swirler configurations ($r/D_t = 9$ and $x/D_t = 1$).

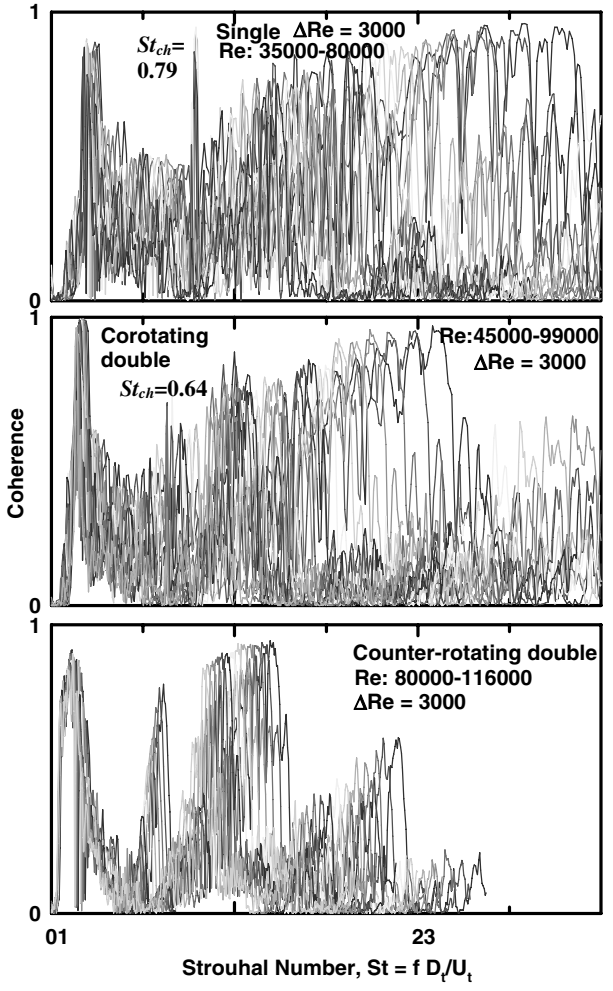

Fig. 11 Coherence of Fig. 10 as a function of the Strouhal number ($r/D_t = 9$ and $x/D_t = 1$).

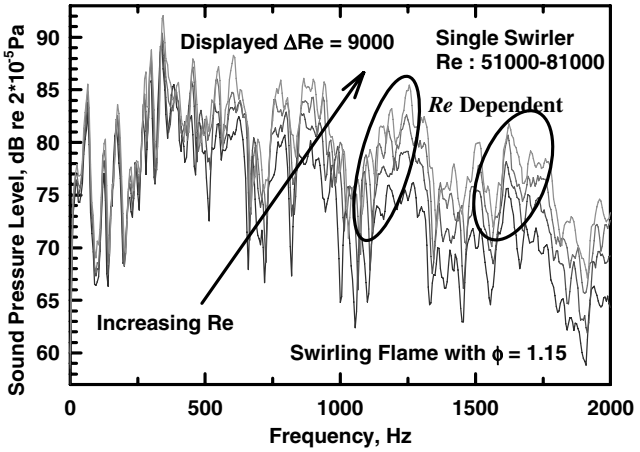

Fig. 12 Effect of Reynolds number variation on the sound pressure spectra of swirling flames with $\Phi = 1.15$ and a constant Reynolds number increment of 3000 ($r/D_t = 9$ and $x/D_t = 1$).

Figure 13 presents comparison of sound pressure spectra of partially premixed swirling flames ($\Phi = 1.15$) with sound pressure spectra of nonreacting swirling flows at $Re = 72,000$. Combustion-generated noise is low-frequency and, thus, the flame spectra have 20–40 dB higher amplitudes in the low-frequency region, up to 1000 Hz. In fact, the spectral levels of flames and flows are comparable at frequencies higher than 1300 Hz, suggesting that there is no contribution from the combustion noise sources in that frequency range. However, the amplitudes at PVC frequencies for single and corotating double-swirler flows are higher than the amplitudes in the flame spectra. The swirling flame with single and corotating double-swirler configurations generate very similar spectra in the low-frequency region (up to 500 Hz), with the highest spectral amplitude at around 325 Hz. However, counter-rotating double-swirler flames generate very different plateaulike spectra in low-frequency region (up to 500 Hz), with the highest spectral amplitude at around 175 Hz. The velocity field of swirling flows with counter-rotating swirlers is very different from those of single and corotating double swirlers, leading to different noise sources [9,10]. At the same Φ and Reynolds number, the corotating double-swirler flame generates the least sound, whereas the counter-rotating flame is the noisiest.

Figure 14 depicts the comparison of plenum pressure fluctuations spectra of swirling flames ($\Phi = 1.15$) with plenum pressure fluctuations spectra of nonreacting swirling flows at $Re = 72,000$. The spectra of the flames and flows for all swirler configurations are very similar, except for the tone at 100 Hz that was observed in the corotating double-swirler flow. Therefore, the presence of flames does not influence the plenum pressure fluctuations. The flow rate establishes the excitation of natural modes and is unaffected by the presence of the flame downstream. Figure 15 presents a comparison of the coherence between the plenum pressure fluctuations and sound pressure for swirling flames and flows, using all three configurations. Unlike swirling flows, the natural modes of the plenum are not transmitted downstream in swirling flames. This provides an insight into the transfer function across the swirling combustion zone and may be useful from a combustion dynamics perspective.

Figure 16 shows sound pressure frequency spectra for swirling nonreacting flows and swirling premixed flames with an equivalence

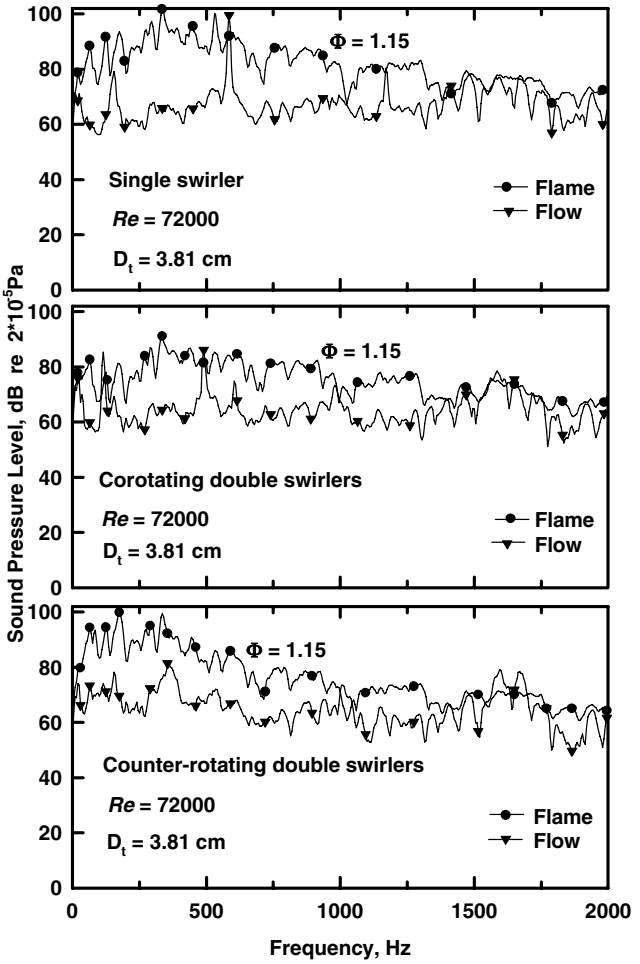

Fig. 13 Comparison of sound pressure spectra of swirling flames ($\Phi = 1.15$) with sound pressure spectra of nonreacting swirling flows for three swirler configurations at $Re = 72,000$ ($r/D_t = 9$ and $x/D_t = 1$).

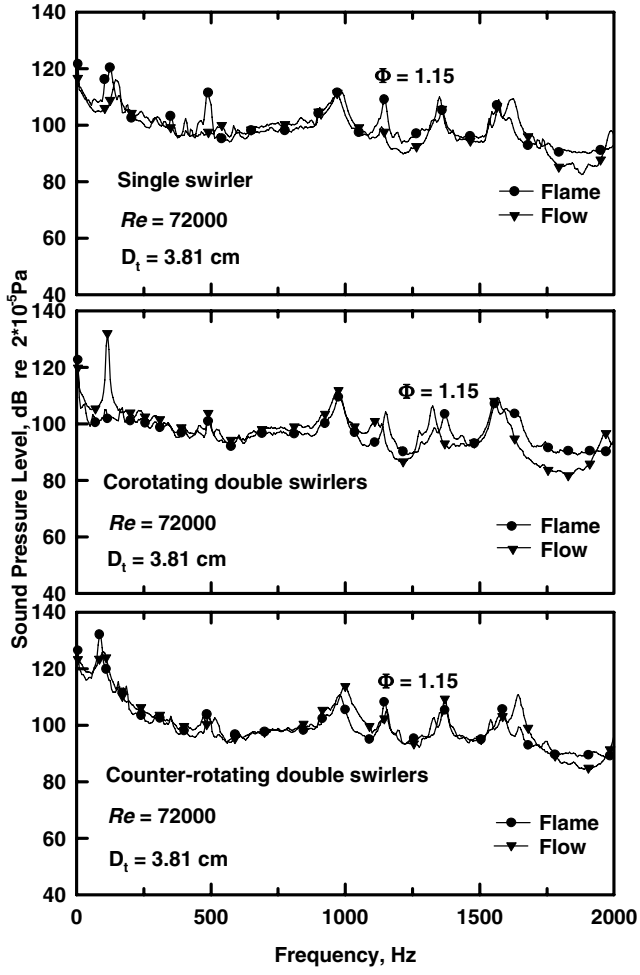

Fig. 14 Comparison of plenum pressure fluctuations spectra of swirling flames ($\Phi = 1.15$) with plenum pressure fluctuations spectra of nonreacting swirling flows for three swirler configurations at $Re = 72,000$ ($r/D_t = 9$ and $x/D_t = 1$).

ratio Φ of 0.98, for three different swirler configurations: single, co-, and counter-rotating double swirlers. Even in current lean premixed systems, the center nozzle may operate at an equivalence ratio of around 0.85–0.95. For the ATS premixer, this equivalence ratio is chosen by design. The bandwidth was 10 kHz, the frequency resolution was 25 Hz, and the sampling frequency was 25.6 kHz. These measurements were obtained by maintaining an identical pressure drop of 2.5% of the atmospheric pressure across the swirler premixer, as practiced in the gas turbine industry. All nonreacting swirling flows exhibit highly tonal spectra, due to the PVC. Previous flow velocity measurements [9] for this experimental apparatus (at the same operating condition, using an identical pressure drop for the measurements and comparison) showed that the mean velocity fields of single and corotating double swirlers are very similar, whereas the velocity field of counter-rotating double swirlers is substantially different. Both single and corotating double swirlers generated a large internal recirculation zone, which is reduced drastically for the counter-rotating configuration; this is probably responsible for the substantial differences observed between the noise emissions of the different swirlers. Merkle et al. [43] have reported that counterswirl does not affect the shape and size of the outer recirculation zone, whereas the internal recirculation zone is strongly influenced by the orientation of the swirl and is shorter in the presence of a counterswirl. The differences observed in the spectra probably originate from the internal recirculation zone. Nevertheless, the counter-rotating double swirlers produce the highest flow rate among the configurations investigated, with the lowest sound pressure amplitude at the PVC frequency. For swirling premixed flames,

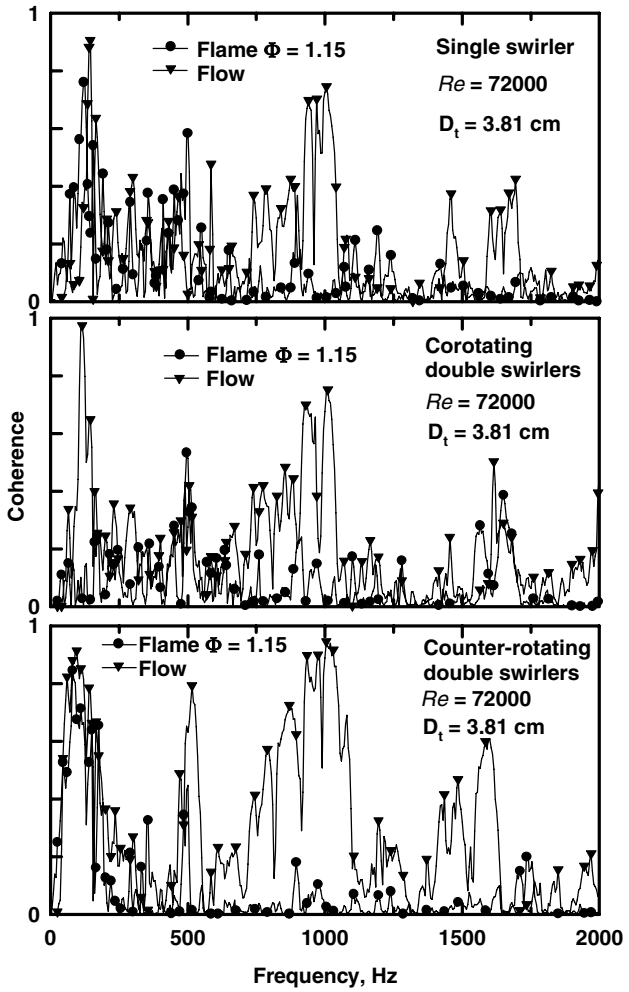

Fig. 15 Comparison of coherence between plenum pressure fluctuations and sound pressure of swirling flames (Φ = 1.15) with coherence between plenum pressure fluctuations and sound pressure of nonreacting swirling flows for three swirler configurations at $Re = 72,000$ ($r/D_t = 9$ and $x/D_t = 1$).

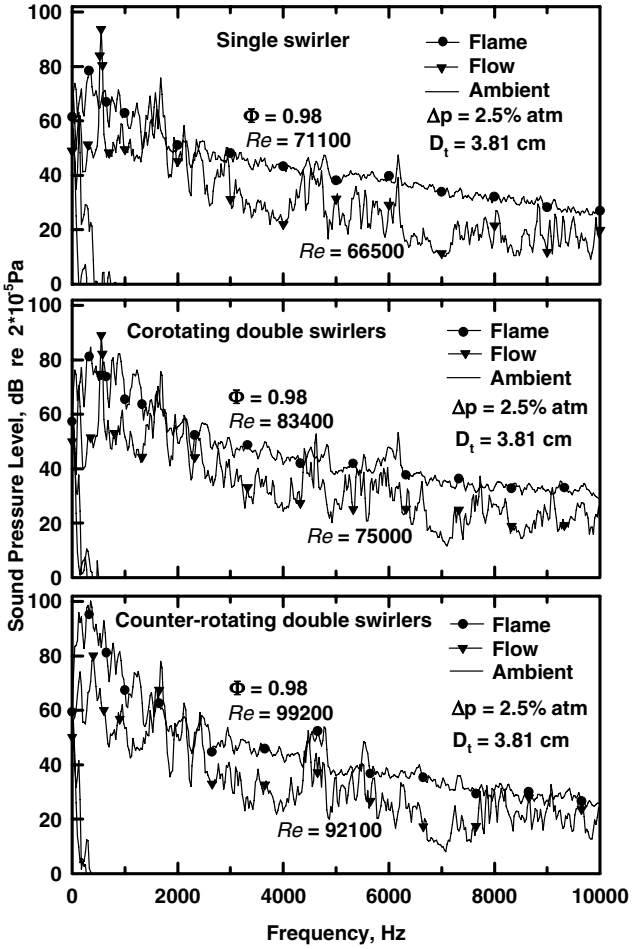

Fig. 16 Comparison of sound pressure spectra generated by swirling flames and flows with $\Delta p = 2.5\%$ atm with three swirler configurations ($r/D_t = 9$ and $x/D_t = 1$).

spectral levels increase in the order of single, co-, and counter-rotating double-swirler configurations. Corotating double-flame spectra are similar to the single-swirl flame, with higher amplitudes. However, in the counter-rotating double-swirler flame, the sound intensity in the frequency range of less than 600 Hz is substantially greater than for the single- and corotating double-swirling flames. At higher frequencies, the spectral level of the counter-rotating double-swirler flame drops to the levels of the corotating double- and single-swirl flames. Both single and corotating double-swirler flames produced broadband spectra without strong evidence of a PVC; however, the counter-rotating double-swirler flame produced tonal spectra with greater amplitudes than those related to the PVC in the nonreacting flow. This suggests a possible enhancement of the PVC. A similar observation that the counterswirl amplifies three-dimensional instability has been made using charge-coupled device (CCD) images of co- and counterswirling flames [22].

Conclusions

The following can be concluded from the current study:

1) The sound spectra of nonreacting swirling flows are dominated by tonal components generated by the PVC. The PVC influences the internal plenum pressure fluctuations spectra, and natural modes of plenum affect the external sound spectra.

2) At identical Reynolds number and Mach number, for swirling nonreacting flows, the PVC frequency, the spectral amplitude at that PVC frequency, and the OASPL are the highest for the single swirler, followed by the co- and counter-rotating double swirlers, respectively.

3) For swirling nonreacting flows, the rates of increase in the PVC frequency and OASPL with the Reynolds number and Mach number

are the highest for the single swirler, followed by the co- and counter-rotating double swirlers, respectively.

4) Double swirlers exhibit dual PVC frequencies, indicating a lack of complete mixing.

5) The presence of a second swirler slows down the PVC and acts as a barrier to the upstream transmission of the PVC and the transmission of plenum pressure fluctuations to the external sound field, with counter-rotation having a stronger impact than corotation.

6) Under identical operating conditions, swirling flames produce higher overall sound pressure than nonreacting swirling flow. However, the OASPL generated by the nonreacting swirling flows exhibits a higher rate of increase, with increase in Mach number, compared with the OASPL generated by swirling flames.

7) At the same Φ and Reynolds number, corotating swirling flames are the least noisy, whereas counter-rotating swirling flames are the noisiest.

8) Swirling flames inhibit the transmission of high-frequency tones across them.

9) For identical pressure differential across swirlers, swirling a premixed flame with counter-rotating double swirlers generates a higher OASPL than a similar flame with corotating double swirlers, which produces more OASPL than the single-swirler flame.

Acknowledgments

We gratefully acknowledge Gabriel Roy, Office of Naval Research (ONR), for supporting the present work through grant number N00014-02-1-0769 and Jun Ji, School of Mechanical Engineering, Purdue University, for his help with the present study.

References

[1] Syred, N., and Beer, J. M., "Combustion in Swirling Flows: A Review," *Combustion and Flame*, Vol. 23, No. 2, 1974, pp. 143–201.

[2] Lilley, D. G., "Swirl Flows in Combustion: A Review," *AIAA Journal*, Vol. 15, No. 8, 1977, pp. 1063–1078.

[3] Gupta, A. K., Lilley, D. G., and Syred, N., *Swirl Flows*, Abacus Press, Tunbridge Wells, England, U.K., 1984.

[4] Lefebvre, A. H., *Gas Turbine Combustion*, 2nd ed., Taylor and Francis, Philadelphia, 1999.

[5] Cheng, R. K., "Velocity and Scalar Characteristics of Premixed Turbulent Flames Stabilized by Weak Swirl," *Combustion and Flame*, Vol. 101, Nos. 1–2, 1995, pp. 1–14.

[6] Fick, W., Griffiths, A. J., O'Doherty, T., Syred, N., and Froud, D., "Phase Averaged Temperature Characterization in Swirl Burners," *Proceedings of the Institution of Mechanical Engineers*, Part A, Vol. 210, No. 5, 1996, pp. 383–395.

[7] Fick, W., Griffiths, A. J., and O'Doherty, T., "Visualization of the Precessing Vortex Core in an Unconfined Swirling Flow," *Optical Diagnostics in Engineering*, Vol. 2, No. 1, 1997, pp. 19–31.

[8] Meier, W., Keck, O., Noll, B., Kunz, O., and Stricker, W., "Investigations in the TECFLAM Swirling Diffusion Flame: Laser Raman Measurements and CFD Calculations," *Applied Physics B (Lasers and Optics)*, Vol. 71, No. 5, 2000, pp. 725–731.

[9] Ji, J., and Gore, J. P., "Combustion Instabilities in An Advanced Turbine System Premixer," 37th AIAA/ASME/SAE/ASEE Joint Propulsion Conference and Exhibit, Salt Lake City, Utah, AIAA Paper 2001-3852, 2001.

[10] Ji, J., and Gore, J. P., "Flow Structure in lean Premixed Swirling Combustion," *Twenty-Ninth (International) Symposium on Combustion*, Combustion Inst., Pittsburgh, PA, 2002, pp. 861–867.

[11] Anacleto, P. M., Fernandes, E. C., Heitor, M. V., and Shtork, S. I., "Characterization of a Strong Swirling Flow with Precessing Vortex Core Based on Measurements of Velocity and Local Pressure Fluctuations," *11th International Symposium on Applications of Laser Technique to Fluid Mechanics* [CD-ROM], Calouste Gulbenkian Foundation, London 2002; also available at http://in3.dem.ist.utl.pt/lxlaser2002/papers.asp [retrieved 16 Dec. 2006].

[12] Keck, O., Meier, W., Stricker, W., and Aigner, M., "Establishment of a Confined Swirling Natural Gas/Air Flame as a Standard Flame: Temperature and Species Distributions from Laser Raman Measurements," *Combustion Science and Technology*, Vol. 174, No. 8, 2002, pp. 117–151.

[13] Kulshmeimer, C., and Buchner, H., "Combustion Dynamics of Turbulent Swirling Flames," *Combustion and Flame*, Vol. 131, Nos. 1–2, 2002, pp. 70–84.

[14] Lucca-Negro, O., and O'Doherty, T., "Vortex Breakdown: A Review," *Progress in Energy and Combustion Science*, Vol. 27, No. 4, 2001, pp. 431–481.

[15] Froud, D., O'Doherty, T., and Syred, N., "Interaction of the Precessing Vortex Core and Reverse Flow Zone in the Exhaust of a Swirl Burner," *Proceedings of the Institution of Mechanical Engineers*, Part A, Vol. 208, No. 1, 1994, pp. 27–36.

[16] Syred, N., and Beer, J. M., "The Damping of Precessing Vortex Cores by Combustion in Swirl Generators," *Acta Astronautica*, Vol. 17, Nos. 4–5, 1972, pp. 783–801.

[17] Syred, N., and Beer, J. M., "Effect of Combustion Upon Precessing Vortex Cores Generated by Swirl Combustors," *Fourteenth (International) Symposium on Combustion*, Combustion Inst., Pittsburgh, PA, 1973, pp. 537–550.

[18] Syred, N., Gupta, A. K., and Beer, J. M., "Temperature and Density Gradient Changes Arising with the Precessing Vortex Core and Vortex Breakdown in Swirl Burners," *Fifteenth (International) Symposium on Combustion*, Combustion Inst., Pittsburgh, PA, 1974, pp. 587–597.

[19] Froud, D., O'Doherty, T., and Syred, N., "Phase Averaging of the Precessing Vortex Core in a Swirl Burner under Piloted and Premixed Combustion Conditions," *Combustion and Flame*, Vol. 100, No. 3, 1995, pp. 407–412.

[20] Syred, N., Fick, W. O'Doherty, T., and Griffiths, A. J., "The Effect of the Precessing Vortex Core on Combustion in a Swirl Burner," *Combustion Science and Technology*, Vol. 125, Nos. 1–6, 1997, pp. 139–157.

[21] Gupta, A. K., Lewis, M. J., and Qi, S., "Effect of Swirl on Combustion Characteristics of Premixed Flames," *Journal of Engineering for Gas Turbines and Power*, Vol. 120, No. 3, 1998, pp. 488–494.

[22] Gupta, A. K., Lewis, M. J., and Daurer, M., "Swirl Effects on Combustion Characteristics of Premixed Flames," *Journal of Engineering for Gas Turbines and Power*, Vol. 123, No. 3, 2001, pp. 619–626.

[23] Syred, N., Wong, C., Rodriquez-Martinez, V., Dawson, J., and Kelso, R., "Characterization of the Occurrence of the Precessing Vortex Core in Partially Premixed and Non-Premixed Swirling Flow," *12th International Symposium on Applications of Laser Technique to Fluid Mechanics* [CD-ROM], Calouste Gulbenkian Foundation, London, 2004; also available at http://in3.dem.ist.utl.pt/LXLASER2004/program.asp [retrieved 16 Dec. 2006].

[24] Culick, F. E. C., "Combustion Instabilities in Propulsion Systems," *Combustion Instabilities Driven by Thermo-Chemical Acoustics Sources*, edited by A. S. Hersh, I. Catton, and R. F. Kelite, Vol. 128, Heat Transfer Div., and Vol. 4, Noise Control and Acoustics Div., American Society of Mechanical Engineers, New York, 1989, pp. 33–52.

[25] Lieuwen, T. C., Torres, H., Johnson, C., and Zinn, B. T., "A Mechanism of Combustion Instability in Lean Premixed Gas Turbine Combustors," *Journal of Engineering for Gas Turbines and Power*, Vol. 123, No. 1, 2001, pp. 182–188.

[26] Lawn, C. J., "Interaction of the Acoustic Properties of a Combustion Chamber with Those of Premixture Supply," *Journal of Sound and Vibration*, Vol. 224, No. 5, 1999, pp. 785–808.

[27] Syred, N., Hanby, V. I., and Gupta, A. K., "Resonant Instabilities Generated by Swirl Burners," *Journal of the Institute of Fuel*, Dec. 1973, pp. 402–407.

[28] Strahle, W. C., "On Combustion Generated Noise," *Journal of Fluid Mechanics*, Vol. 49, No. 2, 1971, pp. 399–414.

[29] Strahle, W. C., "Combustion Noise," *Progress in Energy and Combustion Science*, Vol. 4, No. 3, 1978, pp. 157–176.

[30] Chiu, H. H., and Summerfield, M., "Theory of Combustion Noise," *Acta Astronautica*, Vol. 1, Nos. 7–8, 1974, pp. 967–984.

[31] Crighton, D. G., Dowling, A. P., Ffowcs-Williams, J. E., Heckl, M., and Leppington, F. G., *Modern Methods in Analytical Acoustics: Lecture Notes*, Springer–Verlag, London, 1992, pp. 378–403.

[32] Gupta, A. K., Syred, N., and Beer, J. M., "Fluctuating Temperature and Pressure Effects on the Noise Output of Swirl Burners," *Fifteenth (International) Symposium on Combustion*, Combustion Inst., Pittsburgh, PA, 1975, pp. 1367–1377.

[33] Bertrand, C., and Michelfelder, S., "Experimental Investigation of Noise Generated by Large Turbulent Diffusion Flames," *Sixteenth (International) Symposium on Combustion*, Combustion Inst., Pittsburgh, PA, 1976, pp. 1757–1769.

[34] Gupta, A. K., Syred, N., and Beer, J. M., "Noise Sources in Swirl Burners," *Applied Acoustics*, Vol. 9, No. 2, pp. 151–163, 1976.

[35] Gupta, A. K., Syred, N., and Beer, J. M., "On Combustion Generated Noise from Turbulent Diffusion Gaseous Flames," *Applied Acoustics*, Vol. 11, No. 1, 1978, pp. 35–55.

[36] Hardalupas, Y., and Selbach, A., "Imposed Oscillations and Non-Premixed Flames," *Progress in Energy and Combustion Science*, Vol. 28, No. 1, 2002, pp. 75–104.
[37] Neemeh, R., Algattus, S., and Neemeh, L., "Experimental Investigation of Noise Reduction in Supersonic Jets Due to Jet Rotation," *Journal of Sound and Vibration*, Vol. 221, No. 3, 2000, pp. 505–524.
[38] Nair, S., and Lieuwen, T. C., "Acoustic Detection of Imminent Blowout In Pilot And Swirl Stabilized Combustors," 2003 ASME Turbo Expo, Atlanta, GA, International Gas Turbine Inst., Paper GT2003-38074, 2003.
[39] Toqan, M. A., Beer, J. M., Jansohn, J., Sun, N., Testa, A., Shihadeh, A., and Teare, J. D., "Lox NO_x-Emissions from Radially Stratified Natural Gas-Air Turbulent Diffusion Flames," *Twenty-Fourth (International) Symposium on Combustion*, Combustion Inst., Pittsburgh, PA, 1992, pp. 1391–1399.
[40] Terasaki, T., and Hayashi, S., "The Effects of Fuel-Air Mixing on NO_x Formation in Non-Premixed Swirl Burners," *Twenty-Sixth (International) Symposium on Combustion*, Combustion Inst., Pittsburgh, PA, 1996, pp. 2733–2739.
[41] Ateshkadi, A., McDonell, V. G., and Samuelson, G. S., "Effect of Hardware Geometry on Gas and Drop Behavior in a Radial Mixer Spray," *Twenty-Seventh (International) Symposium on Combustion*, Combustion Inst., Pittsburgh, PA, 1998, pp. 1985–1992.
[42] Merkle, K., Büchner, H., Zarzalis, N., and Sara, O. N., "Influence of Co- and Counter Swirl on Lean Stability Limits of an Airblast Nozzle," 2003 ASME Turbo Expo, Atlanta, GA, International Gas Turbine Inst., Paper GT2003-38004, 2003.
[43] Merkle, K., Haessler, H., Buchner, H., and Zaralis, N., "Effect of Co- and Counter-Swirl on the Isothermal Flow- and Mixture-Field of an Airblast Atomizer Nozzle," *International Journal of Heat and Fluid Flow*, Vol. 24, No. 4, 2003, pp. 529–537.
[44] Marshall, A. W., and Gupta, A. K., "Effects of Jet Momentum Distribution on Thermal Characteristics of Co-Swirling Flames," 34th AIAA Aerospace Sciences Meeting, Reno, NV, AIAA Paper 96-0404, 1996.
[45] Weisbrod, W. D., Jr., "Allison Engine Company's Industrial Advanced Turbine Systems Program Overview" *National Energy Technology Laboratory* [online archive], http://www.netl.doe.gov/publications/proceedings/97/97ats/ats_pdf/ATS2-1.PDF [retrieved 16 Dec. 2006].
[46] Singh, K. K., "An Experimental Study of the Effects of Partial Premixing and Swirler Configuration on Noise Generated by Turbulent Jet and Swirling, Flows and Flames," Ph.D. Thesis, Purdue Univ., West Lafayette, IN, May 2005.
[47] Shivashankara, B. N., Strahle, W. C., and Handley, J. C., "Combustion Noise Radiation by Open Turbulent Flames," *Aeroacoustics: Jet and Combustion Noise, Duct Acoustics*, edited by H. T. Nagamatsu, Vol. 37, Progress in Astronautics and Aeronautics, AIAA, New York, 1975, pp. 277–296.
[48] Singh, K. K., Frankel, S. H., and Gore, J. P., "Effects of Combustion on the Sound Pressure Generated by Circular Jet Flows," *AIAA Journal*, Vol. 41, No. 2, 2003, pp. 319–321.
[49] Morse, P. M., and Ingard, K. U., *Theoretical Acoustics*, Princeton Univ. Press, Princeton, NJ, 1968, pp. 509–511.
[50] Pierce, A. D., *Acoustics: An Introduction to Its Physical Principles and Applications*, Acoustical Society of America, Woodbury, NY, 1991, pp. 315–316.
[51] Singh, K. K., Frankel, S. H., and Gore, J. P., "A Study of Spectral Noise Emissions from Standard Turbulent Non-Premixed Flames," *AIAA Journal*, Vol. 42, No. 5, 2004, pp. 931–936.

S. Aggarwal
Associate Editor